

## **Additively manufactured Haynes 230 by laser powder directed energy deposition (LP-DED): effect of heat treatment on microstructure and tensile properties**

Muztahid Muhammad<sup>1,2</sup>, Reza Ghiaasiaan<sup>1,2</sup>, Paul R. Gradl<sup>3</sup>, Shuai Shao<sup>1,2</sup>, Nima Shamsaei<sup>1,2\*</sup>

<sup>1</sup>National Center for Additive Manufacturing Excellence (NCAME), Auburn University, Auburn, AL 36849, USA

<sup>2</sup>Department of Mechanical Engineering, Auburn University, Auburn, AL 36849, USA

<sup>3</sup>NASA Marshall Space Flight Center, Propulsion Department, Huntsville, AL 35812, USA

\*Corresponding author:  
shamsaei@auburn.edu  
Phone: (334) 844-4839

### **Abstract**

The microstructure and tensile mechanical properties of Haynes 230 fabricated through laser powder directed energy deposition (LP-DED) were investigated, varying temperature heat treatments between 900°C to 1177°C following deposition. Scanning electron microscopy (SEM) was employed for microstructural analysis, whilst tensile testing was utilized to evaluate the room temperature mechanical properties of the alloy. In an as-deposited state, the initial microstructure consisted of cellular  $\gamma$  and  $M_6C/M_{23}C_6$  carbides. The cellular regions seem to be fully dissolved upon solutionizing at 1177°C for 3 hours. Following post-deposition heat-treatments, the carbides were observed to precipitate and grow along the grain boundaries as well as in the interior of grains. Solutionizing at 1177°C for 3 hours following stress-relieving yielded better ductility and had an insignificant effect on the strength.

**Keywords:** Laser powder directed energy deposition, Haynes 230, microstructure, tensile behavior.

### **Introduction**

Haynes 230 is a solid solution and carbide strengthening nickel-base superalloy with high-temperature mechanical strength and corrosion resistance. This alloy is used in many aerospace applications, therefore a potential candidate for applications such as hot sections for gas turbines, heat exchangers of nuclear reactors, etc.[1]. However, machining of Haynes 230 alloy is a challenge, especially for components with complex geometries. Additive manufacturing (AM), a layer-by-layer manufacturing technology, has the capability to fabricate complex parts in near-net-shape conditions with none to minimal machining requirements. Among different AM processes, laser powder directed energy deposition (LP-DED) is a well-known AM process where injected powder particles are melted together by a laser heat source and are deposited into the melt pool [2].

Although AM offers numerous benefits, there are challenges associated due to AM

parts' unique thermal histories, such as rapid melting and solidification, leading to different microstructure compared to the conventionally fabricated parts as well as induced residual stress and volumetric defects [3]. Consequently, the mechanical properties of AM parts may differ from their conventionally manufactured counterparts. Hence, the microstructure and mechanical properties of AM parts need to be studied before the implementation of heat treatments designed for wrought materials.

In general, as-fabricated AM Ni-base superalloys consist of cellular inter-dendritic structures that affect mechanical properties compared to conventionally fabricated counterparts. Solid solution and carbide strengthened Ni-base superalloys fabricated using both wrought [4] and AM [5] processes are known for their superior ductility. Since solid solution strengthened Ni-base superalloys such as Haynes 230 do not possess detrimental Nb in their chemical composition like precipitation strengthened Ni-base superalloys, the Haynes 230 has the potential to improve the ductility by post-process homogenization (or partial removal) of the initial micro-segregation and inter-dendritic structure induced during the prior AM fabrication process with a minimal negative effect on strengths. Although Haynes 230 alloy has been studied in conventionally processed [1,4,6–8] and AM conditions [9,10], there is a lack of knowledge for the effect of multiple-step heat treatment processes on subsequent mechanical properties of AM Haynes 230 alloy. In this study, the effect of different heat treatments on the microstructure and tensile properties of LP-DED Haynes 230 is investigated. Tensile behaviors of LP-DED Haynes 230 at various heat treatment conditions are correlated with their corresponding microstructure.

### **Experimental Procedure**

The Haynes 230 test specimens were fabricated using the RPM Innovations (RPMI) 557 LP-DED system using the process parameters tabulated in **Table 1**. Powders used to fabricate the Haynes 230 specimens were supplied by Praxair Surface Technologies, Inc., and the chemical composition of powders is listed in **Table 2**. The AM test specimens were machined to a final geometry of tensile specimens according to ASTM E8 standard [11], as shown in **Figure 1**. Prior to the final machining, the tensile test specimens were heat treated using a 'Sentro tech high-temperature tube furnace' with a heating rate of 5°C/minute. To investigate the effect of prior stress-relieving (SR), the specimens were stress-relieved (SR) at two different temperatures, i.e., 900°C and 1066°C for 1.5 hours, followed by solutionizing at 1177°C for 3 hours, as shown in **Figure 2** and **Table 3**. The suggested range of solution treatment for wrought Haynes 230 alloy is from 1177°C to 1246°C [4,12–14].

Microstructural analyses were performed on small coupons cut from heat treated test specimens, in the plane perpendicular to the build direction. The microstructural coupons were later mounted and ground, and polished according to ASTM-E3 [15]. A Zeiss Crossbeam 550 scanning electron microscope (SEM) equipped with energy dispersive spectroscopy (EDS) and Electron backscatter diffraction (EBSD) detectors were used for further microstructural analysis. Backscattered secondary electron (BSE) micrographs were obtained using the electron channeling contrast imaging (ECCI) technique [16].

Quasi-static monotonic tensile testing was conducted utilizing an MTS landmark

servo-hydraulic machine with a load cell of 100 KN. Three tensile specimens were tested for each heat treated condition. An extensometer was used for accurate yield strength measurement during tensile testing. However, for the limited displacement range of the extensometer, the tensile test was conducted in two stages. The extensometer was attached to the surface of the specimen only up to the first 0.05 mm/mm strain of the tensile test. After removal of the extensometer, the remaining test was conducted in displacement-controlled mode until fracture.

**Table 1.** Process parameters used in this study for fabrication of the LP-DED Haynes 230 specimens.

Power (W)	Layer height ( $\mu\text{m}$ )	Travel speed (mm/min)	Powder feed rate (g/min)
1070	381	1016	19.10

**Table 2.** Chemical composition of LP-DED Haynes 230 powders used in this study.

Elements	Wt. %
Ni	Bal.
C	0.1
Mn	0.56
Si	0.55
P	<0.01
S	<0.001
Cr	20.72
Mo	1.94
W	14.12
Al	0.47
La	0.012
Co	<0.01
Ti	0.04
B	<0.001
Fe	0.14
Cu	0.01

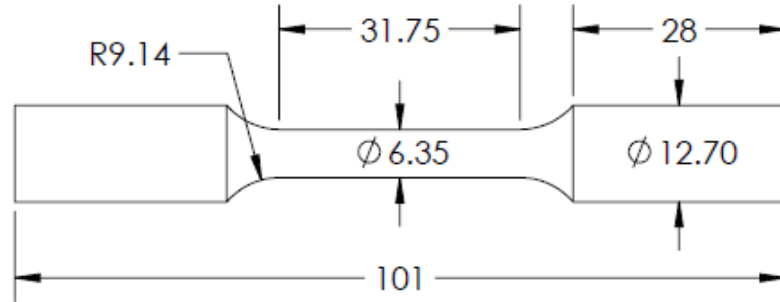


**Figure 1.** Tensile specimen geometry of LP-DED Haynes 230 (All dimensions are in mm).

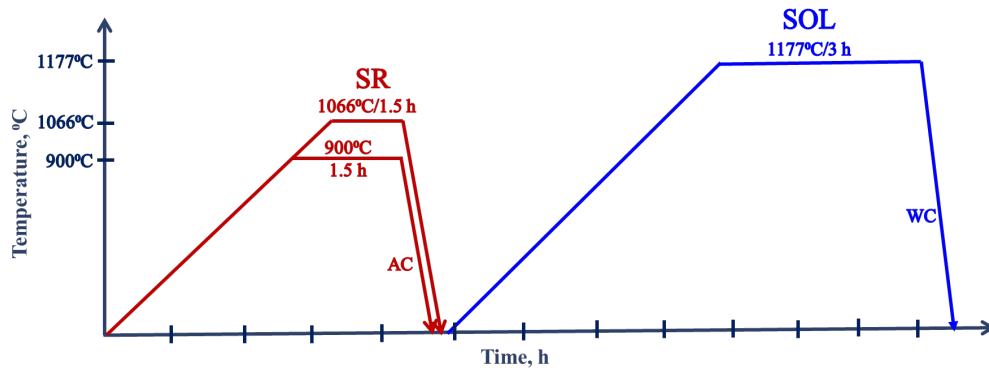


**Figure 2.** Diagram presenting heat treatments conducted on LP-DED Haynes 230 in this study.

**Table 3.** Heat treatments (with designations) conducted on LP-DED Haynes 230 in this study.

Heat treatment	Step 1 (Stress-relieving)			Step 2 (Solutionizing)			Designation
	Temperature (°C)	Time (hr)	Cooling	Temperature (°C)	Time (hr)	Cooling	
As-built	None	None	None				Non-heat treated (NHT)
Stress-relieved	900°C	2	Air (AC)	None	None	None	900-None
	1066°C			None	None	None	1066-None
Stress-relieved + Solutionized	900°C	2	Air (AC)	1177°C	3	Water (WC)	900-1177
	1066°C			1066-1177			

## **Results and Discussion**

Inverse pole figure (IPF) maps obtained from EBSD analysis for all heat treatment conditions are presented in **Figure 3** along with their grain size distribution in the plane perpendicular to the build direction. As shown, typical fine equiaxed grains are observed in the non-heat treated (NHT) condition. Furthermore, some ultra-fine grain regions are also discernible in the EBSD map, which could be ascribed to the inhomogeneous formation of grain boundary carbides pinning the growth of the ultra-fine grains. These carbides are indeed effective in resisting grain growth as there are not much recrystallization and grain growth observed even after further heat treatments, as shown in **Figure 3**. Note that it is expected that the NHT condition has more small grains which gradually grow during heat treatment even though it is indicated otherwise in **Figure 3(f)**. These grains may be too small for the IPF mapping to capture at the magnification used (i.e., the probe points have a much higher probability to be near grain boundaries), which led to a higher fraction of zero solutions during EBSD analysis.

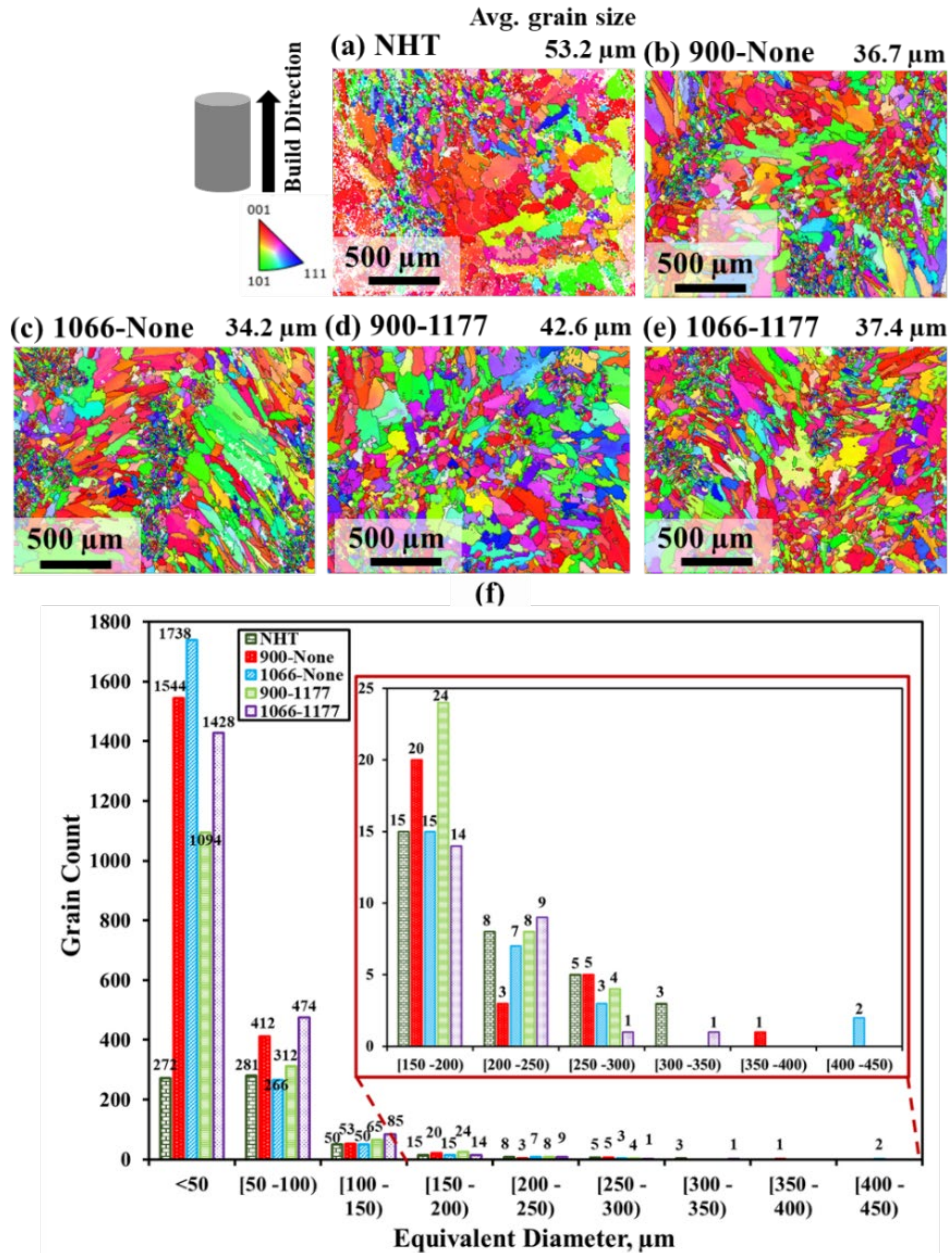


**Figure 3.** Inverse pole figure (IPF) maps of LP-DED Haynes 230 in the plane perpendicular to the build direction for different heat treated conditions: (a) NHT, (b) 900-None, (c) 1066-None, (d) 900-1177, and (e) 1066-1177; (f) Grain size distribution of LP-DED Haynes 230 for different heat treated conditions

The higher resolution, BSE micrographs for all heat treatments investigated are presented in **Figure 4**. It can be seen that the NHT DED Haynes 230 consists of cellular dendritic microstructure with severe micro-segregation in the  $\gamma$  matrix, as shown in **Figures 4(a)-(b)**, which is consistent with the reported data in the literature [9]. Typically, cellular interdendritic network in the AM materials can increase the strengths at the cost of the ductility. Formation of some filmy carbides along the inter-dendritic regions is also observed at the

NHT LP-DED Haynes 230 (indicated by red arrows in **Figure 4(b)**). Chemical composition observed by EDS analysis in Haynes 230 indicates the presence of Mo-rich and Cr-rich carbides (as shown in **Figure 5**), which may be Mo-rich ( $M_6C$ ) and Cr-rich ( $M_{23}C_6$ ) carbides typical for Haynes 230 and is consistent reports in the literature [8,9]. Carbides also can contribute to the high-temperature strengthening mechanism in the Haynes 230 by resisting the grain boundary sliding at high temperatures [17].

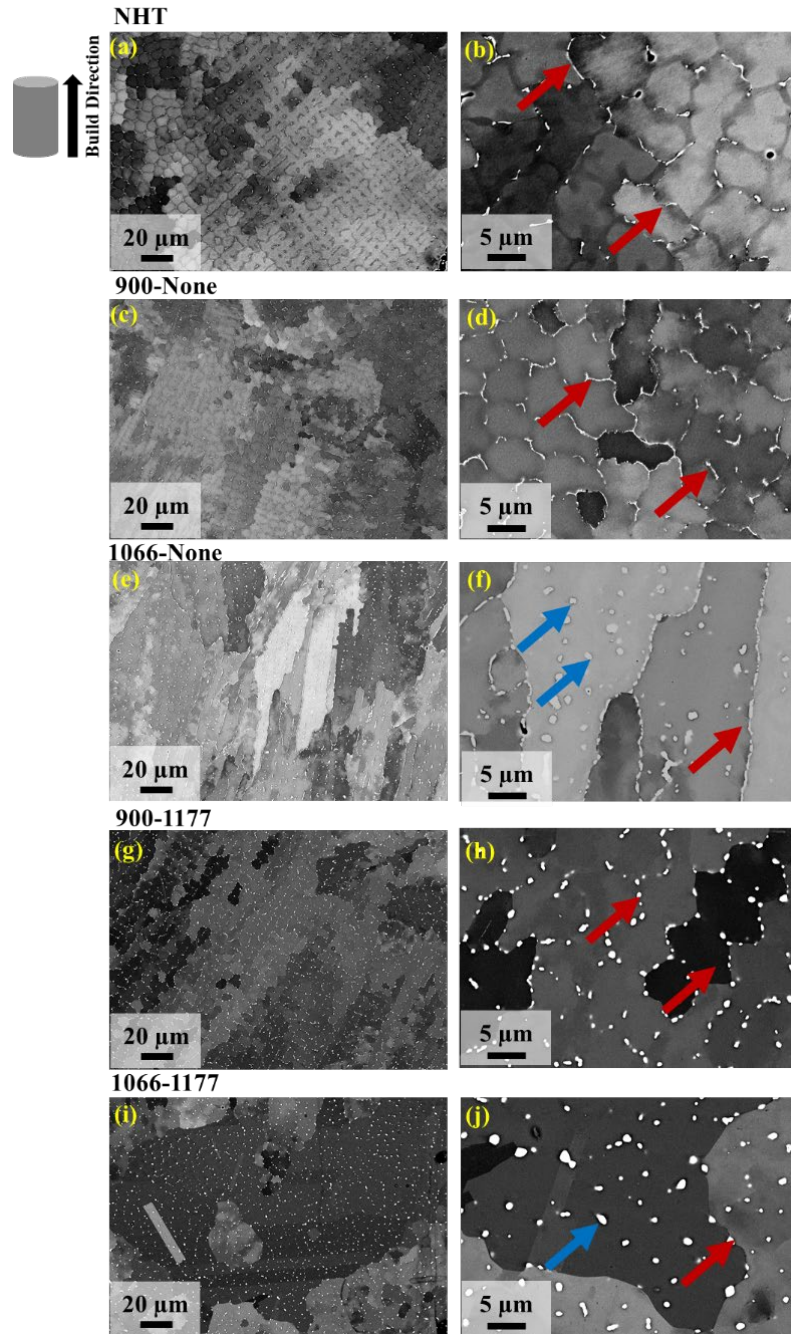


**Figure 4.** Typical BSE micrographs obtained in the plane perpendicular to build direction for various heat treated conditions of the LP-DED Haynes 230: (a)-(b) NHT, (c)-(d) 900-None, (e)-(f) 1066-None, (g)-(h) 900-1177, and (i)-(j) 1066-1177. Red and



blue arrows point to the carbides formed at grain boundaries and grain interior regions, respectively.

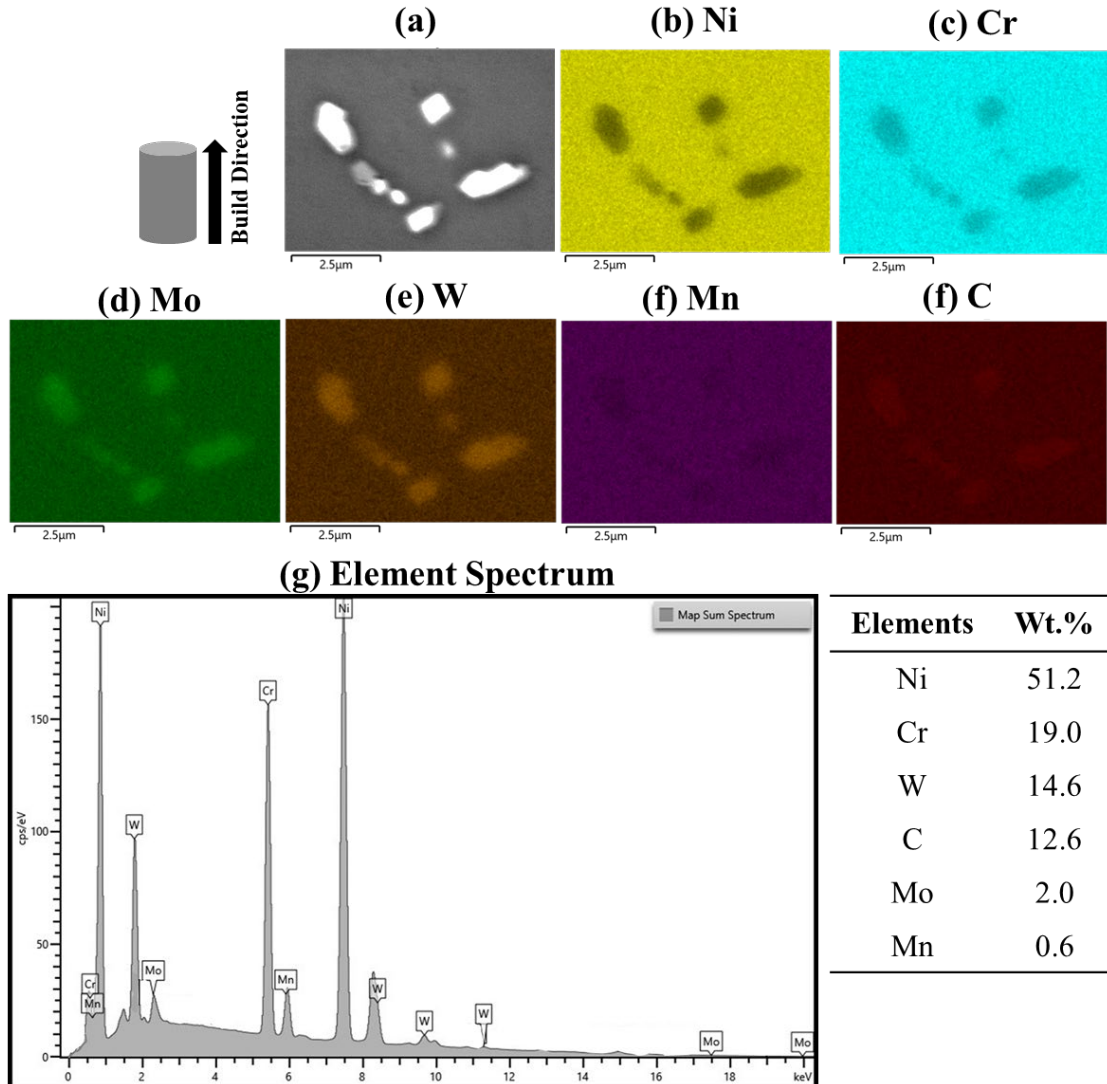


**Figure 5.** Typical elemental maps and the overall chemical content from EDS for the 1066-1177 solution treated LP-DED Haynes 230 specimen in the plane perpendicular to the build direction.

Upon the low-temperature 1-step heat treatment (or SR) at 900°C (900-None), the micro-segregations at the inter-dendritic regions are dissolved and permitted the formation of more filmy carbides at these locations, as shown in **Figures 4(d)**. For the wrought Haynes 230 [8], large carbides (i.e.,  $M_6C$ ) start dissolving at temperature 600°C, and smaller  $M_{23}C_6$  carbides start forming in grain interior regions. These small carbides forming with the grain interior regions could play as a minor strengthening source for the alloy [17].

On the other hand, upon the high-temperature 1-step heat treatment (or SR) at 1066°C (1066-None), the inter-dendritic regions are more significantly dissolved as compared to the low-temperature SR at 900°C (900-None), as shown in **Figures 4(e)-(f)**. It is also notable that in 1066-None specimens, the grain boundary and inter-dendritic carbides



have become more globular and the number density of the carbides in the grain interior regions are increased (carbides at grain interior regions are indicated by blue arrows in **Figure 4(f)**), which could be ascribed to the prior inter-dendritic carbides that were dissolved after heat treatment or diffusion of elements at the grain interior regions. Furthermore, it seems that the 2-step heat treatment (or solution treatment) at 1177°C could completely remove the inter-dendritic regions, as shown in **Figures 4(g)-(j)**. It should be noted that, upon 2-step heat treatment (or solution treatment) at 1177°C, (900-1177 and 1066-1177), the grain boundary carbides tend to become discrete and spheroidize (See **Figures 4(h)** and **(j)**).

Engineering stress-engineering strain and engineering stress-displacement curves of LP-DED Haynes 230 in various heat treatment conditions investigated in this study are shown in **Figures 6(a)** and **(b)**, respectively. In addition, **Figure 7** presents the comparative column charts for uniaxial tensile properties, including yield strength ( $S_y$ ), ultimate tensile strength ( $S_u$ ), and percent elongation (%EL) of LP-DED Haynes 230 investigated in this study with and those of laser powder bed fusion (L-PBF) [10] and wrought [4] counterparts found in the literature.

As shown in **Figure 6** and **Figure 7**, upon the 1-step heat treatment (or SR), the elongation has not significantly changed as compared with the NHT condition (~36-38%). However, the higher temperature 1-step heat treatment (or SR) at 1066°C (1066-None) has lowered the yield strength (~353 MPa) as compared with the NHT conditions (~433 MPa), whereas the SR at 900°C (900-None) has not significantly affected the yield strength (~431 MPa). This could be ascribed to the effect of 1-step heat treatment on microstructure. As shown in **Figures 4(c)-(d)**, the lower temperature 1-step heat treatment (900-None) has partially removed the micro-segregation within the prior inter-dendritic regions and formed more carbides in the grain interior. These carbides can lead to more pronounced dislocation multiplication and greater strain hardening (compare the curves for NHT and 900-None in **Figure 6(b)**). On the other hand, the higher temperature 1-step heat treatment (1066-None) not only succeeded in complete dissolution of prior micro-segregation but also could partially remove the prior inter-dendritic regions. In addition, some carbides formed within the grain interior regions. Therefore, the lower yield strength after the high-temperature 1-step heat treatment (1066-None) could be attributed to the partial removal of the inter-dendritic structures, as shown in **Figures 4(c)-(d)**, which could play as impediments for the dislocations' motion during deformation [5].

Furthermore, upon the 2-step heat treatment at 1177°C, the uniaxial tensile properties were comparable with a slight increase in ductility. This could be attributed to the homogenization effect of high-temperature 2-step heat treatment on the microstructure where the carbides formed at grain boundary and grain interior regions have appeared in a more circular morphology, and almost all the prior inter-dendritic regions are removed.

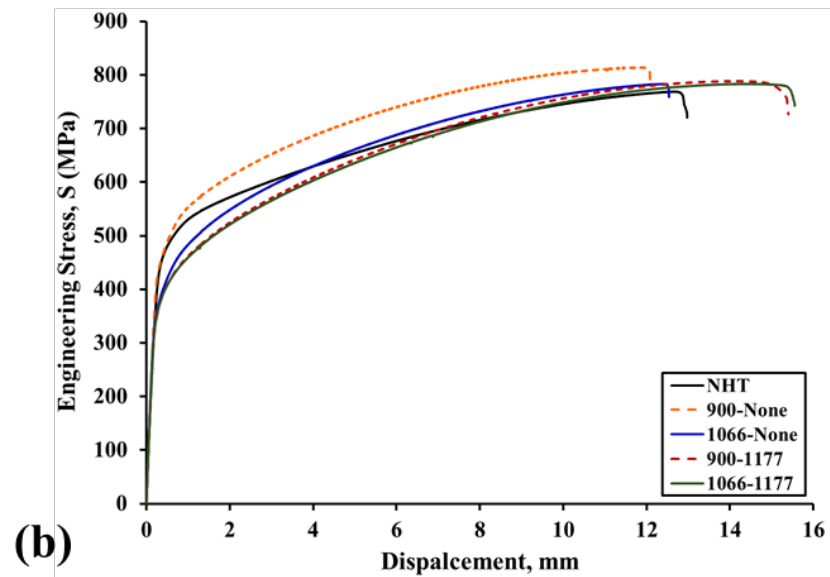
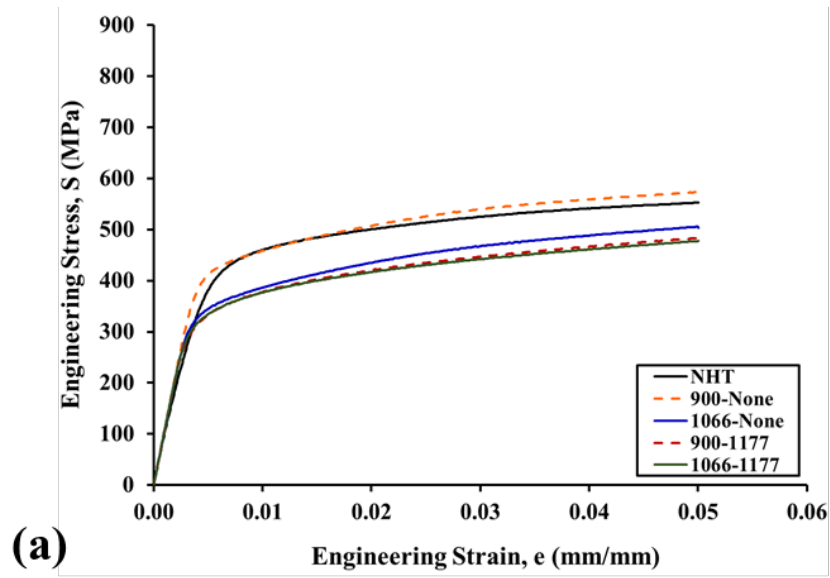


**Figure 6.** Tensile behavior of LP-DED Haynes 230 alloy: (a) engineering stress-engineering strain curves, and (b) engineering stress-displacement curves.

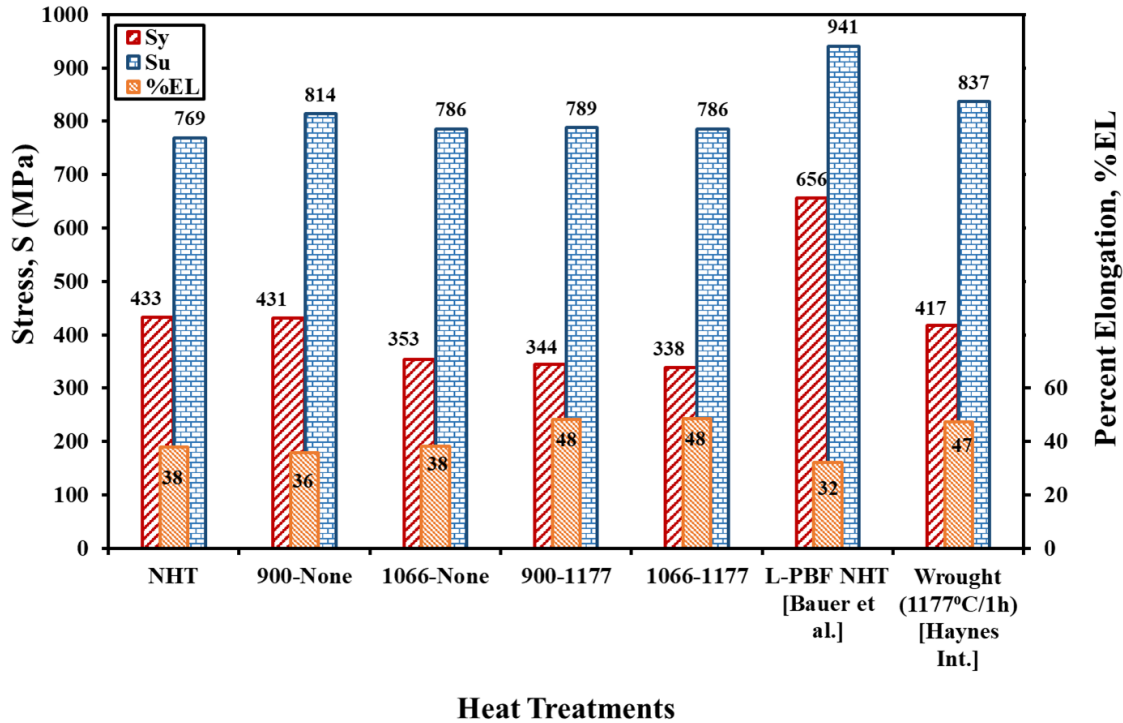


**Figure 7.** Column chart presenting tensile properties of LP-DED Haynes 230 alloy investigated in this study as well as L-PBF [10] and wrought [4] Haynes 230 alloys from literature.

### Summary and Conclusions

In this study, the microstructure and tensile behavior of LP-DED Haynes 230 alloy after various multiple steps heat treatments were investigated. The tensile behavior of each heat treatment was characterized and discussed in relation to their microstructure. The effect of hot isostatic pressing (HIP) in the microstructure and mechanical properties of AM Haynes 230 alloy will be explored in the future. The following conclusions can be drawn from this study:

- The microstructural results revealed that the low-temperature 1-step heat treatment (SR) at 900°C has partially dissolved the prior micro-segregation with insignificant effect on the inter-dendritic regions while the carbides formed at grain boundaries become more discrete and continuous at grain boundary areas. On the other hand, the higher temperature 1-step heat treatment (SR) at 1066°C has not only removed almost all the prior micro-segregation but also partially dissolve the prior inter-dendritic structure.
- Upon the high-temperature 2-step heat treatment (or solution treatment) at 1177°C, the microstructure has become more homogenized with the partial dissolution of the inter- dendritic regions as well as the formation of discrete carbides at grain interior and boundary areas.
- The tensile results of the low-temperature 1-step heat treatment (SR) at 900°C showed comparable properties with non-heat treated (NHT) conditions which could

be attributed to the minimal effect of heat treatment on prior inter-dendritic regions, which could play as impediments for dislocation motions. On the other hand, the high-temperature 1-step heat treatment (SR) at 1066°C has lowered yield strength due to partial removal of inter-dendritic regions.

- The 2-step heat treatment at 1177°C, the tensile properties are more comparable regardless of prior 1-step heat treatment, which could be attributed to the homogenization effect of the 2-step heat treatment at 1177°C on microstructure where the inter-dendritic regions are partially removed while the carbides are formed at the grain boundary and interior regions in a more circular shape.

### **Acknowledgment**

This material is partially supported by the National Aeronautics and Space Administration NASA under Cooperative Agreement No. 80MSFC19C0010. This paper describes objective technical results and analysis. Any subjective views or opinions that might be expressed in the paper do not necessarily represent the views of the National Aeronautics and Space Administration (NASA) or the United States Government.

### **References**

- [1] C.J. Boehlert, S.C. Longanbach, A comparison of the microstructure and creep behavior of cold rolled HAYNES® 230 alloy™ and HAYNES® 282 alloy™, *Mater. Sci. Eng. A.* 528 (2011) 4888–4898.
- [2] M. Molitch-Hou, Overview of additive manufacturing process, *Addit. Manuf.* (2018) 1–38.
- [3] A. Yadollahi, N. Shamsaei, Additive manufacturing of fatigue resistant materials: Challenges and opportunities, *Int. J. Fatigue.* 98 (2017) 14–31.
- [4] HAYNES® 230® alloy, 2021.
- [5] R. Ghiaasiaan, M. Muhammad, P.R. Gradl, S. Shao, N. Shamsaei, Superior tensile properties of Hastelloy X enabled by additive manufacturing, *Mater. Res. Lett.* 9 (2021) 308–314.
- [6] K. Hrutkay, Evolution of Microstructure of Haynes 230 and Inconel 617 Under Mechan, 2013.
- [7] D. Kim, I. Sah, C. Jang, Effects of high temperature aging in an impure helium environment on low temperature embrittlement of Alloy 617 and Haynes 230, *J. Nucl. Mater.* 405 (2010) 9–16.
- [8] K. Hrutkay, D. Kaoumi, Tensile deformation behavior of a nickel based superalloy at different temperatures, *Mater. Sci. Eng. A.* 599 (2014) 196–203.
- [9] M. Haack, M. Kuczyk, A. Seidel, E. López, F. Brueckner, C. Leyens, Comprehensive study on the formation of grain boundary serrations in additively manufactured Haynes 230 alloy, *Mater. Charact.* 160 (2020) 110092.
- [10] T. Bauer, K. Dawson, A. Spierings, K. Wegener, Microstructure and mechanical characterisation of SLM processed Haynes® 230®.
- [11] ASTM International, ASTM E8/E8M-16: Standard Test Methods for Tension Testing of Metallic Materials, (2016).
- [12] ASTM F3301, Standard for Additive Manufacturing – Post Processing Methods – Standard Specification for Thermal Post-Processing Metal Parts Made Via Powder

- Bed Fusion, ASTM Stand. (2018) 3.
- [13] H. V Atkinson, S. Davies, Fundamental Aspects of Hot Isostatic Pressing: An Overview, *Metallurgical and Materials Transactions A* 31 (2000) 2981–3000.
  - [14] Hot Isostatic Pressing (HIP) conditions | GE Additive.
  - [15] A.E.– 11 (Reapproved 2017) International, Standard Guide for Preparation of Metallographic Specimens Standard Guide for Preparation of Metallographic Specimens 1, *ASTM Int.* 03.01 (2012) 1–12.
  - [16] S. Zaefferer, N.-N. Elhami, Theory and application of electron channelling contrast imaging under controlled diffraction conditions, *Acta Mater.* 75 (2014) 20–50.
  - [17] On the theory of the effect of precipitate particles on grain growth in metals, *Proc. R. Soc. London. Ser. A. Math. Phys. Sci.* 294 (1966) 298–309.